Journal of Applied Polymer Science

Effects of an Itaconic Acid Comonomer on the Structural Evolution and Thermal Behaviors of Polyacrylonitrile Used for Polyacrylonitrile-Based Carbon Fibers

Zhongyu Fu,[1] Yu Gui,[1] Shuang Liu,[1] Zhe Wang,[1] Baijun Liu,[1] Chunlei Cao,[1] Huixuan Zhang[1,2]

[1]Engineering Research Center of Synthetic Resin and Special Fiber, Ministry of Education, Changchun University of Technology, Changchun 130012, China

[2]Changchun Institute of Applied Chemistry, Chinese Academy of Science, Changchun 130022, China

Correspondence to: C. Cao (E-mail: cao1840@sina.com)

ABSTRACT: The influence of an acid comonomer on the structural evolution and thermal behaviors of a polyacrylonitrile (PAN) terpolymer containing about 4.19 wt % methyl methacrylate and 0.98 wt % itaconic acid (IA) during a heating treatment were studied by Fourier transform infrared (FTIR) spectroscopy, differential scanning calorimetry (DSC), and thermogravimetry (TG) and compared with the PAN homopolymer. From the results of FTIR spectroscopy and DSC, we found that the presence of the IA comonomer promoted cyclization reactions at a faster rate and broadened the exothermic peak; this eased the concentration of heat release. By comparing the results of the TG data, we found that the presence of the IA comonomer promoted dehydrogenation reactions and the formation of a large quantity of better ladder structures. In additional, the better ladder structures that formed were easier to convert from ladder structures into graphitelike structures. The activation energy of random scissions at about 300°C was calculated by the Kissinger method. The results show that the presence of the IA comonomer inhibited the random scission reactions to some extent. © 2014 Wiley Periodicals, Inc. J. Appl. Polym. Sci. **2014**, *131*, 40834.

KEYWORDS: kinetics; spectroscopy; thermal properties; thermogravimetric analysis (TGA)

Received 13 February 2014; accepted 6 April 2014
DOI: 10.1002/app.40834

INTRODUCTION

With the development of the high technology sector, which includes the aerospace and aircraft industries, the demand for carbon fibers, because of their excellent mechanical properties, good chemical and high-temperature inertness, and low weight-to-volume ratios, has increased sharply. Although carbon fibers can obtained be from pitch, rayon, and polyacrylonitrile (PAN), recent studies have established that PAN fibers, which commonly contain a small amount of comonomers, are one of the most suitable and widely applied sources for making high-performance carbon fibers.[1–4]

When PAN fibers are converted into carbon fibers, a heat-treatment stage is needed; this is mostly conducted in an oxidative atmosphere in the temperature range 200–300°C, and a ladderlike structure forms, namely through peroxidation or thermooxidative stabilization.[5–8] Some kinds of chemical reactions take place, primarily dehydrogenation, oxidative cyclization, crosslinking, and random scissions reactions, during this stage. Among them, cyclization reactions, which convert linear PAN into an infusible, stable ladder polymer are of the most importance. However, the cyclization reactions seem to be independent of the atmosphere because they can proceed in either an oxidizing atmosphere or an inert atmosphere. In past decades, many studies[9–16] have been carried out mainly to investigate the mechanisms and kinetics of cyclization, but less attention has been paid to the relationships between cyclization reactions and the degree of the perfection of the formed ladder structures.

As is well known, Fourier transform infrared (FTIR) spectroscopy has been proven to be an excellent technique to study the structures and structural changes of polymers. However, after heat treatment above 300°C in either an inert atmosphere or an oxidizing atmosphere, the PAN polymer becomes infusible and changes from white to black, so not much useful structural information is available from FTIR spectroscopy on carbon fibers, mainly because of the highly absorbing nature of black carbon fibers and the poor resolution of FTIR spectra after high-temperature treatments.[17] Differential scanning calorimetry (DSC) has been widely used to study the thermal behavior of PAN during heat treatment and the kinetic parameters of cyclization reactions, such as the apparent activation energy (E_a) and pre-exponential factor (A), but no useful information on

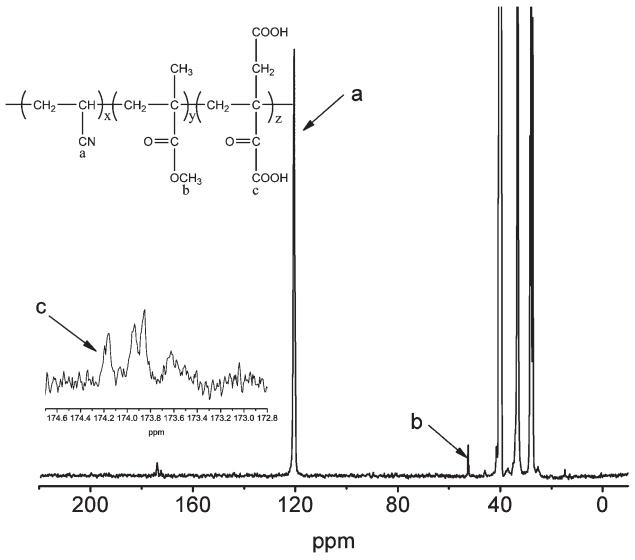

Figure 1. ^{13}C-NMR spectrum of a PAN terpolymer.

structural changes can be deduced from the DSC data. However, it is well known that the thermal stability of PAN at higher temperatures is strongly dependent on the degree of perfection and the amount of ladder structures formed during the heat treatment. We believe that the better stability corresponds to the better perfection and the greater number of ladder structures of PAN, regardless of the atmosphere. So, some useful information about the structural evolution may be inferred from the thermogravimetry (TG) data.

In this study, the composition of P(AN–MMA–IA) terpolymer was analyzed by ^{13}C-NMR. We adapted TG, DSC, and FTIR technologies to study the influence of the acid comonomer on the structural evolution and thermal behaviors of the PAN homopolymer and P(AN–MMA–IA) during heat treatment. An attempt was made to get information about the cyclization reactions from the TG data. The kinetic parameters of the degradation of the PAN polymers at about 300°C were calculated through the TG data. Some new phenomena of kinetics were found, and possible reasons were given to explain the different thermal behaviors.

EXPERIMENTAL

Materials

The PAN homopolymer was prepared by precipitation polymerization in water with ammonium persulfate as the initiator at 50°C under nitrogen. The PAN terpolymer [P(AN–MMA–IA)] fed with about 3 wt % methyl methacrylate (MMA) and 1 wt % itaconic acid (IA) was kindly provided by Jilin Chemical Fibre Co., Ltd. The PAN homopolymer and PAN terpolymer had viscosity-average molecular weights of about 1.75×10^5 and 2.20×10^5, respectively.

Characterization

The ^{13}C-NMR sample was dissolved in deuterated dimethyl sulfoxide (20% w/w polymer solution), and analysis was performed at room temperature in a 5-mm *o.d.* NMR tube with a Bruker Avance III 400 spectrometer operating at 125 MHz with a recycle time of 10 s. To ensure the diffusion of the gas phase, finely powdered samples of the polymers (~5 mg) were used for thermogravimetric analysis (TGA), which was carried out with a PerkinElmer TGA Pyris-1 thermal analyzer in the temperature range between 50 and 600°C in nitrogen at different rates of temperature change, including 5, 7, 10, 15, 20, 30, 40, and 50°C/min. The same weights of finely powdered samples of the polymers were used for DSC analysis with the PerkinElmer DSC Pyris-1 thermal analyzer in the temperature range between 50 and 400°C at 20°C/min in a nitrogen atmosphere. Thin films of the samples were prepared for heat treatment and the following FTIR analysis. The process used was as follows: first, a solution containing about 2 wt % polymer in dimethylformamide was prepared, and then, the dilute solution was cast onto a horizontal glass slice to leave a transparent thin polymer film. Second, the film was extracted in methanol at 50°C for 24 h to remove the residual dimethylformamide. Finally, the film was

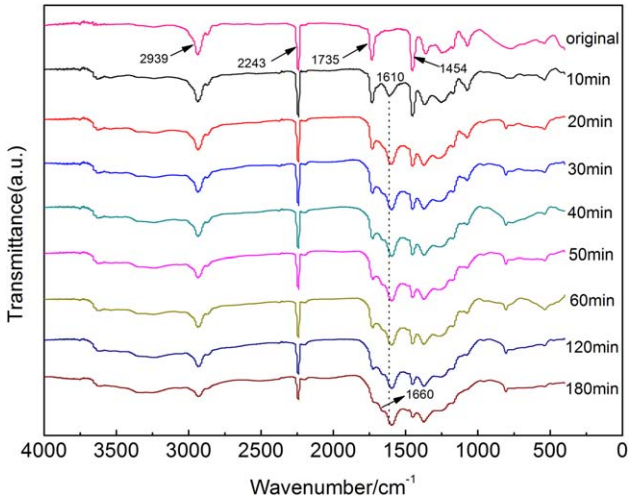

Figure 2. FTIR spectra of P(AN–MMA–IA) heated at 230°C for different times. [Color figure can be viewed in the online issue, which is available at wileyonlinelibrary.com.]

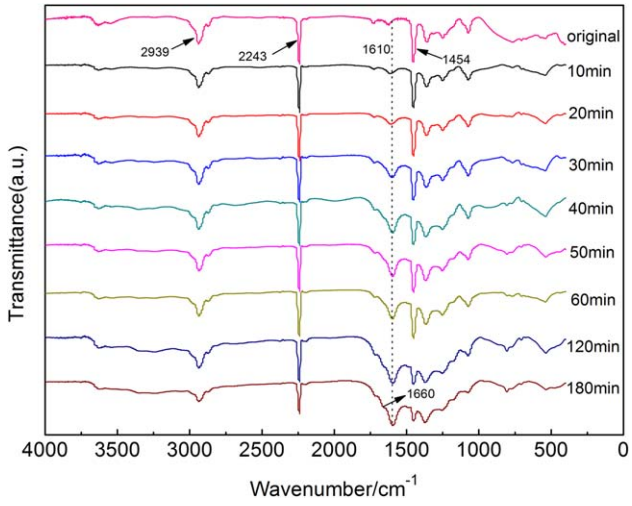

Figure 3. FTIR spectra of PAN heated at 230°C for different times. [Color figure can be viewed in the online issue, which is available at wileyonlinelibrary.com.]

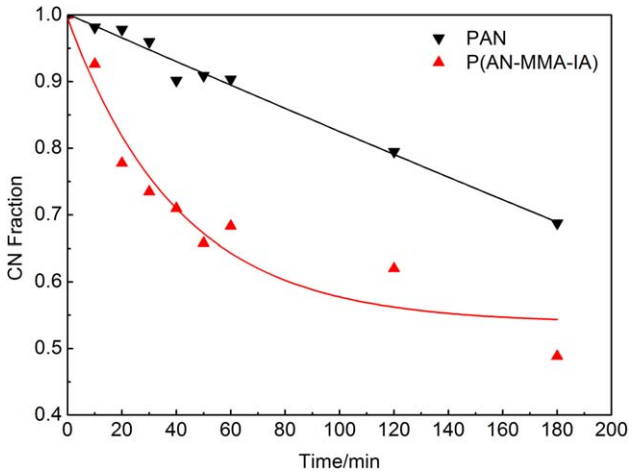

Figure 4. CN fractions of P(AN–MMA–IA) and PAN heated at 230°C for different times. [Color figure can be viewed in the online issue, which is available at wileyonlinelibrary.com.]

dried at 75°C for 24 h *in vacuo* with a thickness about 7 μm. All films were prepared by casting the same volume of the dilute solution onto the same horizontal glass slice. The films for heat treatment were prepared by cutting the dried films to approximately 2 × 2 cm^2. Particular care was taken to remove the nonuniform edges from the cast film and form a usable portion from which heat-treatment samples could be cut. Stabilization was carried out in an air oven at a constant temperature with a temperature accuracy of 1°C.

A Thermo Nicolet Avatar-360 FTIR spectrometer was used to detect structural changes during the heat treatment in the 4000–400-cm^{-1} range at a resolution of 4 cm^{-1}. Then, the extent of the cyclization reactions was calculated by a method reported in a previous work.[18]

RESULTS AND DISCUSSION

Composition of the PAN Terpolymer

A typical ^{13}C-NMR spectrum of the PAN terpolymer is shown in Figure 1. The ratio of the integrations of the nitrile carbons, methyl carbons, and carboxyl carbons (shown by the subscripts *a*, *b*, and *c*, respectively) was used to calculate the compositions with eqs. (1)–(3):

$$f_{(\mathrm{IA})} = \frac{A_{(c)}}{A_{(a)} + A_{(b)} + A_{(c)}} \quad (1)$$

$$f_{(\mathrm{MMA})} = \frac{A_{(b)}}{A_{(a)} + A_{(b)} + A_{(c)}} \quad (2)$$

$$f_{(\mathrm{AN})} = 1 - f_{(\mathrm{IA})} - f_{(\mathrm{MMA})} \quad (3)$$

where $A_{(a)}$, $A_{(b)}$, and $A_{(c)}$ are the area of peaks *a*, *b*, and *c*, as shown in Figure 1, and $f_{(\mathrm{IA})}$, $f_{(\mathrm{MMA})}$, and $f_{(\mathrm{AN})}$ are the molar fractions of IA, MMA, and AN, respectively, in the P(AN–MMA–IA) terpolymer.

The result was that the PAN terpolymer contained 0.98 wt % (IA), 4.19 wt % MMA, and 94.83 wt % AN; this was almost consistent with the feed.

FTIR and DSC Analysis of the Polymers

Figures 2 and 3 give the results of the FTIR spectroscopy of the P(AN–MMA–IA) and PAN, respectively, heated at 230°C in air for different times. Figure 4 shows the extent of P(AN–MMA–IA) and PAN calculated from the results of the FTIR spectroscopy. The assignments of the characteristic absorption bands of P(AN–MMA–IA) and PAN are given as follows:[15,17,19,20] 2939 cm^{-1} (ν_{C-H} in CH_2 or CH_3), 2243 cm^{-1} (ν_{CN}), 1735 cm^{-1} ($\nu_{C=O}$), and 1451 cm^{-1} (δ_{C-H} in CH_2). As illustrated in Figures 2 and 3, the band at 2243 cm^{-1} decreased with increasing heat-treatment time, whereas the band at 1610 cm^{-1} appeared and increased. This was attributed to the combination of C═C and C═N stretching and the N─H in-plane bending of the ladder structures of the stabilized PAN polymer.[15,17,20,21] In addition, a shoulderlike peak at 1660 cm^{-1} was attributed to a conjugated ketone introduced by the hydroxyl oxygen of COOH attacking the carbon atom of an adjacent nitrile group.[15,16,19–22] All of these indicate that the cyclization reactions occurred and progressed to some extent during the heat treatment. However, the difference between Figures 2 and 3 showed that the structural evolution of P(AN–MMA–IA) seemed to be faster than that of PAN. Moreover, the peak at 810 cm^{-1}, due to the out-of-plane bending of C═C─H, appeared and increased as a function of the heat-treatment time. This indicated that the dehydrogenation reaction occurred during the heat treatment. However, the peak at 810 cm^{-1} of P(AN–MMA–IA) occurred at a time of 20 min, whereas the peak at 810 cm^{-1} of PAN occurred at a time of 120 min. In combination with the previous results, we believe that the presence of the IA comonomer also promoted the dehydrogenation reactions. We obtained similar results previously.[23] As shown in Figure 4, that the degree of cyclization reactions of P(AN–MMA–IA) was greater than that of PAN. This showed that the presence of the IA comonomer promoted the formation of a large number of ladder structures. Meanwhile, P(AN–MMA–IA) had a faster cyclization reaction rate than PAN. It is well known that the cyclization mechanism of PAN is a free-radical mechanism (Scheme 1), whereas when the acid comonomers are incorporated into PAN, the mechanism of P(AN–MMA–IA) is an ionic mechanism (Scheme 2) initiated by carboxyl groups.[15,19,22] From the previous results, we observed that the ionic mechanism had an advantage in accelerating and promoting the cyclization reactions at low temperature compared with the radical mechanism. However, information about the degree of perfection of the formed ladder

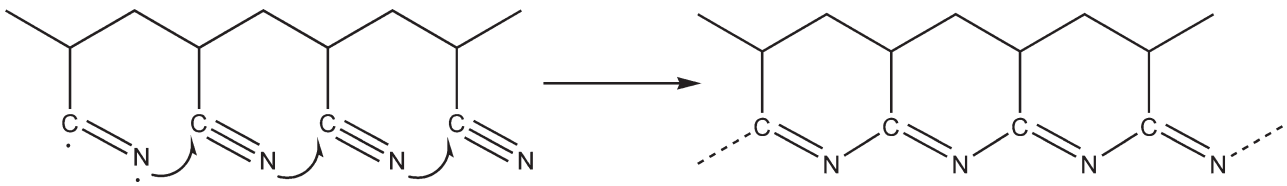

Scheme 1. Cyclization in PAN through a free-radical mechanism.

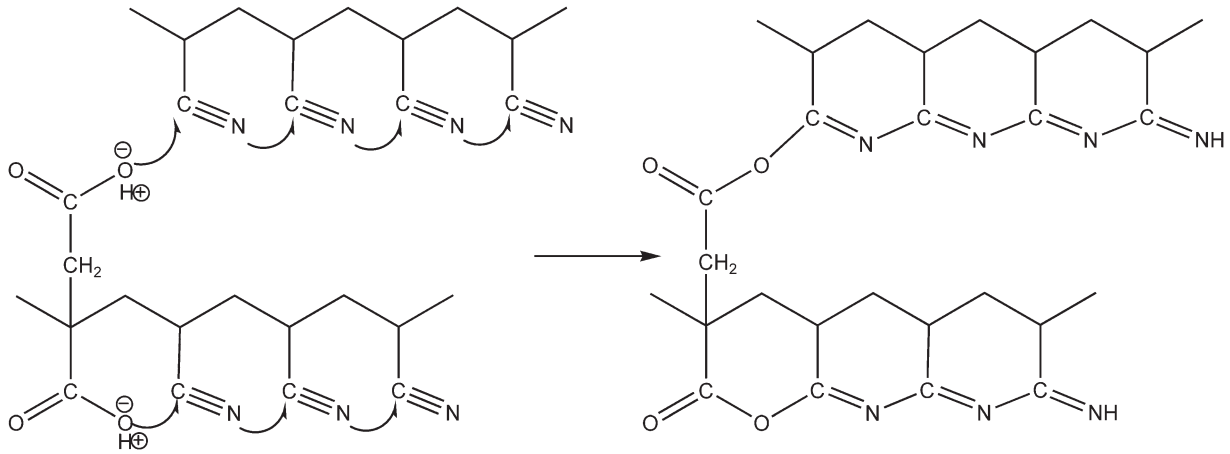

Scheme 2. Cyclization in P(AN–MMA–IA) through an ionic mechanism.

structures could not be obtained from the results of FTIR here. Figure 5 gives the results of the DSC curves of P(AN–MMA–IA) and PAN heated at 20°C/min in an N_2 atmosphere. As shown, the curves of both P(AN–MMA–IA) and PAN exhibited a single exothermic peak, but the curve of P(AN–MMA–IA) was much broader than that of PAN. Moreover, the initiation temperature of the exothermic peak of PAN was at about 280°C; this was about 30°C higher than that of P(AN–MMA–IA). In combination with the results of FTIR spectroscopy, we concluded that the cyclization reactions of P(AN–MMA–IA) were initiated by an ionic mechanism at lower temperature and were faster than those of PAN. It has been established that a large amount of heat to be evolved at the same time will result in the breakage of molecular chains and will give off some kinds of volatile components, and the resulting carbon fiber will have a poor performance.[15,19] So, to produce high-performing carbon fibers, the incorporation of some kind of acid comonomer into PAN is necessary.

TGA of the PAN Polymers Heated at Different Temperature Rates

During all of the TG experiments, about 5 mg of a finely powdered sample was used to ensure the diffusion of gas side productions. The results of the TG curves (mass loss vs temperature) and the derivative thermogravimetric (DTG) curves (mass loss versus temperature) of P(AN–MMA–IA) and PAN heated at 5°C/min are shown in Figures 6 and 7, respectively. From the TG and DTG curves, it was evident that these curves could be roughly divided into three steps according to the extent of weight loss. The first step was up to about 250°C; this weight loss is very small. However, we observed that some weight loss, only about 1 wt %, of P(AN–MMA–IA) occurred earlier than that of PAN; this was attributed to dehydrogenation reactions. The reason for this was that the presence of the IA comonomer promoted the cyclization reactions to form much more thermally stable ladder structures compared to those in PAN. These ladder structures promoted the dehydrogenation to some extent. The results were consistent with the previous FTIR results. The second step was up to about 350°C, where an

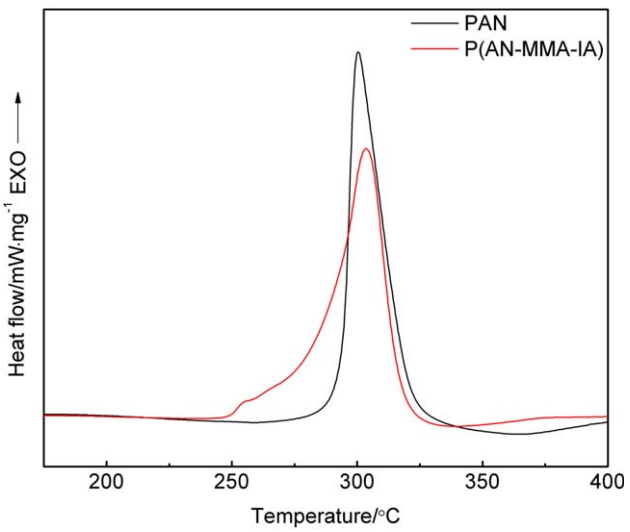

Figure 5. DSC curves of P(AN–MMA–IA) and PAN heated at 20°C/min. [Color figure can be viewed in the online issue, which is available at wileyonlinelibrary.com.]

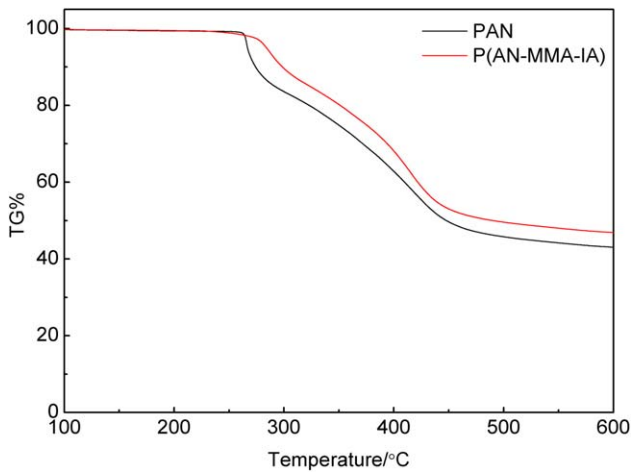

Figure 6. TG curves of P(AN–MMA–IA) and PAN heated at 5°C/min. [Color figure can be viewed in the online issue, which is available at wileyonlinelibrary.com.]

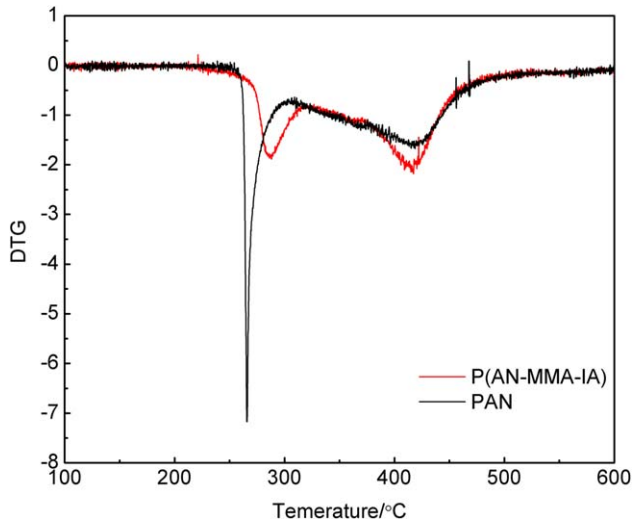

Figure 7. DTG curves of P(AN–MMA–IA) and PAN heated at 5°C/min. [Color figure can be viewed in the online issue, which is available at wileyonlinelibrary.com.]

extensive and very fast weight loss occurred. We believe that the extensive and very fast weight loss was attributed to the vast random scissions of linear PAN chains, which did not participate in the cyclization reactions during the heat treatment. However, it was clear that the random scissions of PAN occurred earlier than those of P(AN–MMA–IA) and had a faster rate; in the meanwhile, the temperature of the highest rate of weight loss of P(AN–MMA–IA) was higher by about 20°C compared to that of PAN. All of these implied that the PAN homopolymer could not form vast and perfect ladder structures by a free-radical mechanism, but the P(AN–MMA–IA) terpolymer could achieve this by an ionic mechanism. So we believe that the tendency of this step indicated the degree of cyclization reactions and perfection of the formed ladder structures. The third step was up to about 500°C. After this step, the TG curves, both of P(AN–MMA–IA) and PAN, reached a retention period; this showed the formation of some more stable structures. As shown in Figures 6 and 7, at the third step, both the P(AN–MMA–IA) and PAN exhibited a relatively fast rate of weight loss; this may have been mainly due to dehydrogenation reactions due to the conversion from ladder structures to graphitelike structures (Scheme 3).[24] However, some differences of the tendency were noticed in that P(AN–MMA–IA) had a faster rate of weight loss than PAN. That is, the conversion from ladder structures to graphitelike structures of P(AN–MMA–IA) was faster and easier than that of PAN.

Figures 8 and 9 show the results of the TG and DTG curves of PAN in nitrogen at different temperature rates. All of the TG and DTG curves showed similar behavior, as stated previously. However, as shown in Figures 8 and 9, as the temperature rate increased, the rate of weight loss around 300°C became faster. That is, as the temperature rate increased, the number of ladder structures forming at 200–300°C decreased; this resulted in the occurrence of vast random scissions of unreacted linear PAN chains and an extensive increase in the rate of weight loss. It was of great interest that the curves obtained at higher temperature rates, such as 30, 40,and 50°C/min, exhibited another maximum rate of weight loss at about 350°C, as shown by the arrow. The reason for this may have been as follows: at high temperature rates, such as 30, 40, and 50°C/min, although some ladder structures formed by the free-radical mechanism, we believe that the formed ladder structures had lots of defects and were less thermally stable. They decomposed at higher temperature, such as 350°C, to some extent, and this increased the weight loss. So, the residual weight at the higher temperature rate was lower, and the residual weight of PAN at 50°C/min was the lowest.

Figures 10 and 11 show the results of the TG and DTG curves of P(AN–MMA–IA) heated at different temperature rates in an N_2 atmosphere. Similar to PAN, with increasing temperature rate, the rate of weight loss became fast; this indicated that although the presence of the IA comonomer promoted the cyclization and dehydrogenation reactions to some extent, not all of the linear PAN chains turned into ladder structures when heat was given. However, through a comparison of Figures 8 and 9 with Figures 10 and 11, we noticed some differences in that at all of the temperature rates, the rate of weight loss of PAN was faster than that of P(AN–MMA–IA). Moreover, the DTG curves of P(AN–MMA–IA) at higher temperature rates

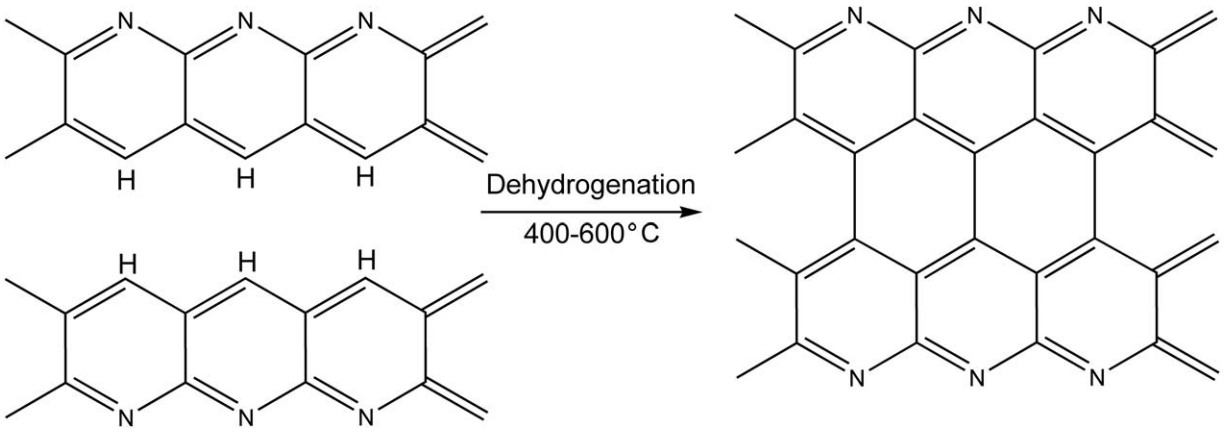

Scheme 3. Dehydrogenation during the conversion from a ladder structure into a graphitelike structure.

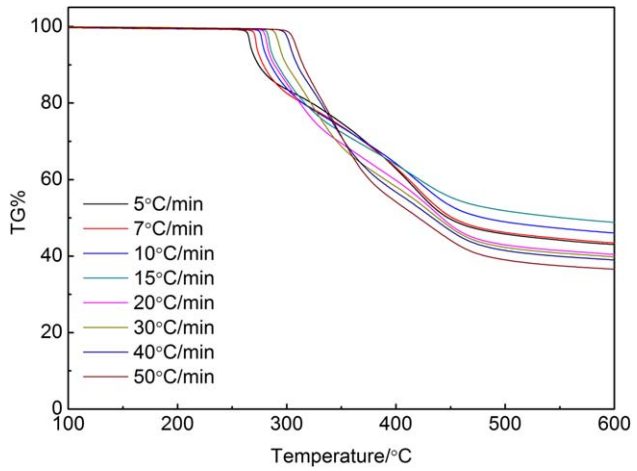

Figure 8. TG curves of PAN heated at different temperature rates. [Color figure can be viewed in the online issue, which is available at wileyonlinelibrary.com.]

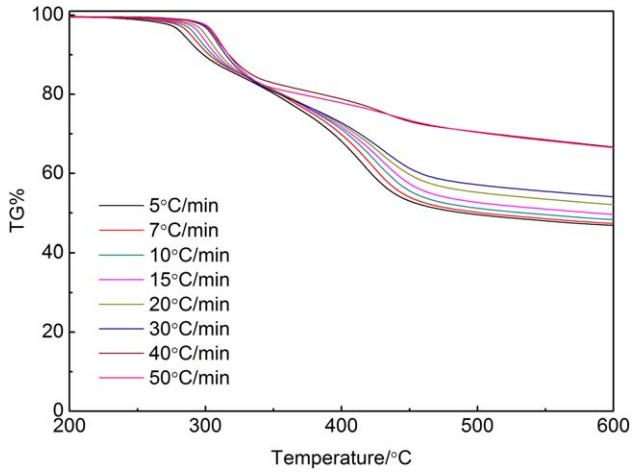

Figure 10. TG curves of P(AN–MMA–IA) heated at different temperature rates. [Color figure can be viewed in the online issue, which is available at wileyonlinelibrary.com.]

did not show a maximum rate of weight loss at 350°C compared to the DTG curves of PAN. All of these indicated that in the same period of time, P(AN–MMA–IA) formed a large number of better ladder structures by the ionic mechanism than PAN through the free-radical mechanism. That is, the ionic mechanism was faster than free-radical mechanism and had the advantage of promoting the formation of more perfect ladder structures. These results were consistent with the results of FTIR spectroscopy stated previously. By comparing the TG results of P(AN–MMA–IA) and PAN heated at 50°C/min, we found that although only about 1 wt % IA comonomer was incorporated into PAN, the weight loss of PAN (~64%) was greater than that of P(AN–MMA–IA) (~33%). This very different thermal behavior demonstrated again that the presence of the IA comonomer promoted the cyclization reactions and inhibited the occurrence of vast random scissions. Moreover, at all temperature rates, the rate of weight loss of P(AN–MMA–IA) at about 450°C was faster than that of PAN, except at rates of 40 and 50°C/min. This also indicated that the ladder structures formed at 200–300°C of P(AN–MMA–AI) were better than those of PAN. This promoted the conversion from ladder structures to graphitelike structures. However, at temperature rates of 40 and 50°C/min, the rate of weight loss of PAN at about 450°C was faster than that of P(AN–MMA–IA), and this seemed confusing. However, the random scissions of chains happened almost continuously throughout the range of 300–600°C, and we believe that the ratio of random scissions of PAN was faster than that of P(AN–MMA–IA) around 450°C. This increased the rate of weight loss of PAN. This may have been the reason why the rate of weight loss of PAN at about 450°C was faster than that of P(AN–MMA–IA).

Evaluation of the E_a Values of Random Scissions in the PAN Polymers

Table I gives the parameters obtained from the DTG curves. The E_a values of the random scissions were determined with the Kissinger method.[25] This method has been mostly adopted to

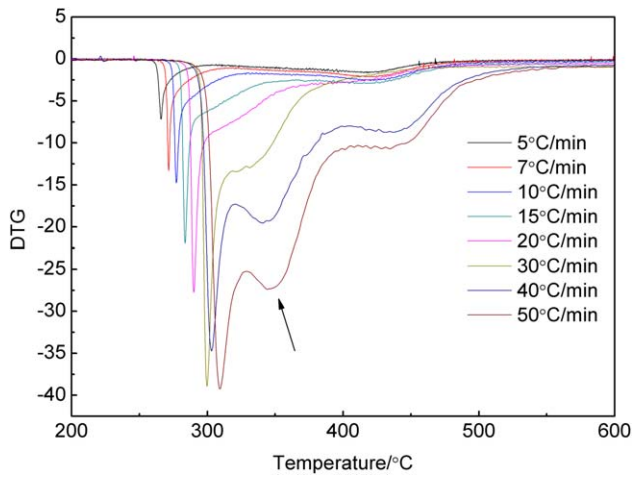

Figure 9. DTG curves of PAN heated at different temperature rates. [Color figure can be viewed in the online issue, which is available at wileyonlinelibrary.com.]

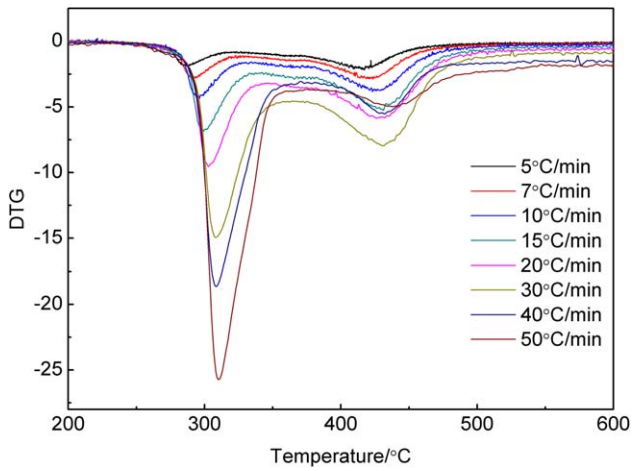

Figure 11. DTG curves of P(AN–MMA–IA) heated at different temperature rates. [Color figure can be viewed in the online issue, which is available at wileyonlinelibrary.com.]

Table I. Parameters for the TG Curves of PAN and P(AN–MMA–IA)

	Rate of temperature change (°C/min)							
	5	7	10	15	20	30	40	50
T_{p1} (°C)[a]	266.0	272.0	277.4	284.0	290.5	300.1	302.8	309.0
T_{p2} (°C)[a]	286.6	290.5	296.2	300.1	302.8	308.1	308.9	310.2

[a] 1, PAN; 2, P(AN–MMA–IA).

calculate E_a in the studies from the literature because no prior knowledge of the reaction mechanism is required to quantify E_a; one only requires a series of TG and DTG curves heated at different rates.

The equation of Kissinger's method is as follows:

$$-\frac{E_a}{R}=\frac{d[\ln(\phi/T_p^2)]}{d(1/T_p)} \quad (4)$$

where T_p is the temperature corresponding to the maximum peak of the DTG curve at a certain heating rate (ϕ). R is the gas constant. E_a is calculated from the slope of the linear plot of $\ln(\phi/T^2_p)$ versus $1000/T_p$, as shown in Figure 12.

The calculated values of E_a are listed in Table II. The E_a values of random scissions for P(AN–MMA–IA) were higher than those for PAN. The higher E_a values showed that the random scissions of P(AN–MMA–IA) were more difficult at the same temperature compared to those of PAN; they also indicate that the incorporation of the IA comonomer in PAN promoted cyclization reactions and formed a large quantity of better ladder structures, as stated previously. In theory, all points calculated from different temperature rates by the Kissinger method should be linear. However, as shown in Figure 12, an interesting discovery was that PAN showed the same behavior theoretically, but P(AN–MMA–IA) did not. The curve of P(AN–MMA–IA) could be divided roughly into two parts. At low rates (≤20°C/min), the curve showed one slope, but at high rates (≥30°C/min), the curve showed another slope. So, we refer to the activation energy of the scissions calculated from the low-temperature rates as E_{a1} and the one calculated from the high-temperature rates as E_{a2}. As shown in Table II, E_{a2} was much higher than E_{a1} by about three times for P(AN–MMA–IA). The possible reasons for this different behavior may be as follows. At low temperature rates, the IA comonomer was consumed wholly to initiate the cyclization reactions before vast numbers of scissions happened. However, at high temperature rates, not all of the IA comonomer was consumed at 200–300°C, and it did not decompose at higher temperatures. So, the residual IA comonomer still initiated the cyclization reactions between the CN groups to form some ladder structures at higher temperatures (e.g., >300°C); this resulted in an increase in the activation energy of scissions. From the previous results, we believe that the TG and DTG curves provided some information about the formed ladder structures at high temperatures, which could not be easily obtained from the FTIR spectra. Moreover, the E_a of random scissions may be a useful parameter in evaluating the degree of cyclization reactions.

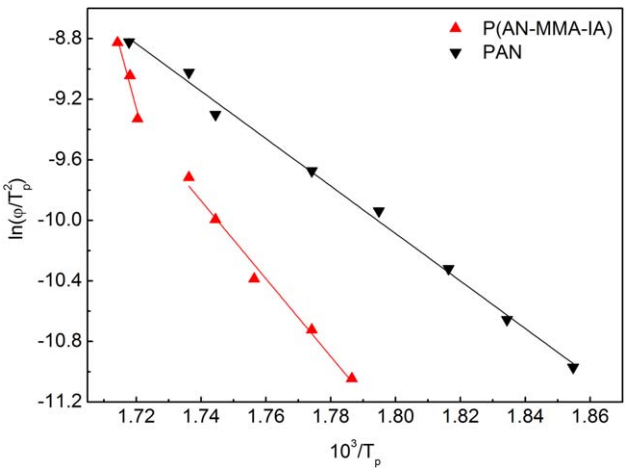

Figure 12. Plots of $\ln(\varphi/T^2_p)$ versus $10^3/T_p$ according to the Kissinger method for PAN and P(AN–MMA–IA). [Color figure can be viewed in the online issue, which is available at wileyonlinelibrary.com.]

CONCLUSIONS

Through FTIR and DSC studies, we found that cyclization reactions between nitriles could be initiated at lower temperatures by the IA comonomer through an ionic mechanism, and the presence of the IA comonomer broadened the DSC exotherm of P(AN–MMA–IA) and eased the sudden heat evolution. In combination with the results of FTIR spectroscopy, TG, and DTG, we inferred that the ionic mechanism was faster than the free-radical mechanism and had an advantage in promoting the formation of a large number of better ladder structures. The TG curves of P(AN–MMA–IA) exhibited a slight weight loss increase at about 250°C; this implied that the dehydrogenation was promoted by the IA comonomer. Moreover, the formed ladder structures promoted the conversion from ladder structures to graphitelike structures. The E_a values of random scissions of PAN and P(AN–MMA–IA) around 300°C were calculated by the Kissinger method. This indicated that the presence of the IA comonomer actually had a kinetic advantage in inhibiting the random scissions at high temperatures. Moreover, the TG and DTG curves provided some information about

Table II. E_a Values Determined by the Kissinger Method

	E_{a1} (kJ/mol)	E_{a2} (kJ/mol)
PAN (N_2)	130.34	130.34
P(AN-MMA-IA) (N_2)	213.00	656.81

the formed ladder structures, which could not be easily obtained from the FTIR spectra. Moreover, the E_a of random scissions may be a useful parameter in evaluating the degree of cyclization reactions.

ACKNOWLEDGMENTS

Financial support of this work from the National Science Foundation of China (contract grant numbers 51073027 and 51273026), the Young Scholar Scientific Foundation of the Science and Technology Department of Jilin Province (contract grant number 20130522140JH), and the Petrochina Innovation Foundation (contract grant number 2013D-5006-0502) is gratefully acknowledged.

REFERENCES

1. Rahaman, M. S. A.; Ismail, A. F.; Mustafa, A. *Polym. Degrad. Stab.* **2007**, *92*, 1421.
2. Xiao, H.; Lu, Y.; Zhao, W.; Qin, X. *J. Mater. Sci.* **2014**, *49*, 794.
3. Park, S. H.; Lee, S. G.; Kim, S. H. *J. Mater. Sci.* **2013**, *48*, 6952.
4. Yu, M. J.; Wang, C. G.; Bai, Y. J.; Zhu, B.; Ji, M. X.; Xu, Y. *J. Polym. Sci. Part B: Polym. Phys.* **2008**, *46*, 759.
5. Bahrami, S. H.; Bajaj, P.; Sen, K. *J. Appl. Polym. Sci.* **2003**, *89*, 1825.
6. Bajaj, P.; Screekumar, T. V.; Sen, K. *J. Appl. Polym. Sci.* **2002**, *86*, 773.
7. Liu, J. J.; Ge, H. Y.; Wang, C. G. *J. Appl. Polym. Sci.* **2006**, *102*, 2175.
8. Devasia, R.; Reghunadhan, N. C. P.; Sadhana, R.; Bab, U. N. S.; Ninan, K. N. *J. Appl. Polym. Sci.* **2006**, *100*, 3055.
9. Coleman, M. M.; Sivy, G. T. *Carbon* **1981**, *19*, 123.
10. Grassie, N.; McGuchan, R. *Eur. Polym. J.* **1970**, *6*, 1277.
11. Xue, Y.; Liu, J.; Liang, J. Y. *Polym. Degrad. Stab.* **2013**, *98*, 219.
12. Beltz, L. A.; Gustafson, R. R. *Carbon* **1996**, *34*, 561.
13. Martin, S. C.; Liggat, J. J.; Snape, C. E. *Polym. Degrad. Stab.* **2001**, *74*, 407.
14. Fitzer, E.; Muller, D. *J. Carbon* **1975**, *13*, 63.
15. Ouyang, Q.; Cheng, L.; Wang, H. J.; Li, K. X. *Polym. Degrad. Stab.* **2008**, *93*, 1415.
16. Park, O. K.; Lee, S.; Joh, H. I.; Kim, J. K.; Kang, P. H.; Lee, J. H.; Ku, B. C. *Polymer* **2012**, *53*, 2168.
17. Zhang, W. X.; Liu, J.; Wu, G. *Carbon* **2003**, *41*, 2805.
18. Collins, G. L.; Thomas, N. W.; Williams, G. E. *Carbon* **1988**, *26*, 671.
19. Ju, A. Q.; Guang, S. Y.; Xu, H. Y. *Carbon* **2013**, *54*, 323.
20. Shimada, I.; Takahagi, T. *J. Polym. Sci. Part B: Polym. Phys.* **1986**, *24*, 1989.
21. Hideto, K.; Kohji, T. *Polym. J.* **1997**, *29*, 557.
22. Bajaj, P.; Screekumar, T. V.; Sen, K. *Polymer* **2001**, *42*, 1707.
23. Fu, Z. Y.; Gui, Y.; Cao, C. L.; Liu, B. J.; Zhou, C.; Zhang, H. X. *J. Mater. Sci.* **2014**, *49*, 2864.
24. Mittal, J.; Konno, H.; Inagakia, M.; Bahlb, O. P. *Carbon* **1998**, *36*, 1327.
25. Kissinger, H. E. *Anal. Chem.* **1957**, *29*, 1702.